

# On the regularization of impact without collision: the Painlevé paradox and compliance

S. J. Hogan and K. Uldall Kristiansen\*

June 17, 2022

## Abstract

We consider the problem of a rigid body, subject to a unilateral constraint, in the presence of Coulomb friction. We focus on the Painlevé paradox known as the inconsistent case where the classic rigid body formalism yields no solution. We regularize the problem by assuming compliance at the point of contact, for a general class of normal reaction force. Using geometric singular perturbation theory and blowup [15, 16], we exploit the fact that the fast solution (or boundary layer) is unstable, by following its unstable direction until the rod sticks. Then we solve the problem both in the stick phase and in the lift off phase. As part of our approach, we show using blowup how solutions obtained by scalings used by previous authors can be matched. We solve the problem for arbitrary values of the compliance damping and give explicit asymptotic expressions in the limiting cases of small and large damping, all for a large class of rigid body.

## 1 Introduction

In mechanics, it has long been known that the rigid body assumption, in problems with unilateral constraints in the presence of friction, can result in the governing equations having multiple solutions (the *indeterminate* case) or no solutions (the *inconsistent* case). The classical example of Painlevé [24, 25, 26], consisting of a slender rod slipping<sup>1</sup> along a rough surface (see Fig. 1), is the simplest and most studied example of these phenomena, now known collectively as *Painlevé paradoxes*. For references to this topic, see the book by Brogliato [4], the review by Stewart [28] or the tutorial paper by Blumenthals *et al.* [2].

For many years, Painlevé's example lay at the margins of mechanics, partly because the coefficient of friction in which these phenomena occurred was considered to be unrealistically large. More recently, it has become clear that such paradoxes can occur at physically realistic

---

\*S. J. Hogan: Department of Engineering Mathematics, University of Bristol, Bristol BS8 1UB, United Kingdom. K. Uldall Kristiansen: Department of Applied Mathematics and Computer Science, Technical University of Denmark, 2800 Kgs. Lyngby, DK.

<sup>1</sup>We prefer to avoid describing this phase of the motion as *sliding* because we will be using ideas from piecewise smooth systems [8], where sliding has exactly the opposite meaning.

parameter values in many systems [18, 19], such as robotic manipulators [32], disc brakes [21], rotating shafts [29, 30] and passive walkers [22, 23].

The classical Painlevé example has been studied in great detail by Génot and Brogliato [9]. They considered dynamics around a critical point, corresponding to zero vertical acceleration of the end of the rod. As well as discovering a new critical value for the coefficient of friction, they also proved that, when starting in a consistent state, the rod must stop slipping before reaching the critical point. In particular, paradoxical situations cannot be reached after a period of slipping.

When a system has no *consistent* solution, it can not remain in that state. Lecornu [17] was the first to propose a jump in vertical velocity to escape an inconsistent, horizontal velocity, state. This jump has been called *impact without collision* [9], *tangential impact* [10] or *dynamic jamming* [23]. The best evidence to support the presence of an impact without collision (IWC) comes from experiments on a two-link manipulator [32]. It was set up in a configuration where no solution to the governing equations was expected, and compelling evidence for an IWC was seen in the data.

To understand how IWC can be incorporated into the rigid body formulation, it is necessary to use methods first proposed by Darboux [6] and Keller [12] in which the differential equations governing the motion are given in terms of the normal impulse, rather than time. However, this process has been controversial [3]. For, in order for IWC to work, it has to occur instantly (since the rod can not exist in the inconsistent state), but the tools available to implement IWC can produce contradictions when used in this setting (such as an apparent energy gain in the presence of friction).

Mathematically, very little work has been done on how the Painlevé paradoxes can be *regularised*. Physically this usually corresponds to assuming some sort of compliance at the contact point  $A$ , typically thought of as a spring, with stiffness and damping that tend to the rigid body model in a suitable limit. Dupont and Yamajako [7] treated the problem as a slow fast system, as we will do. They limited their results to exploring the stability of the fast solution (or boundary layer), which turns out to be unstable for the Painlevé paradoxes. Song *et al.* [27] established conditions under which the fast solution can be stabilized, giving results for also nonlinear compliances and generalized Coulomb friction. They complemented their theoretical work with experimental evidence. Le Suan An [1] considered a system with bilateral constraints and showed that a jump in vertical velocity was obtained from a compliance model with diverging stiffness. But no quantitative results were given and it is not clear how his conclusions apply to the problem shown in Fig. 1. Finally Zhao *et al.* [31] considered the example in Fig. 1 and regularised the equations by assuming a compliance that consisted of an undamped spring. They estimated, as a function of the stiffness, the orders of magnitude of the time taken for the rod to slip in one direction and come to a halt, the time taken to stick and the time to slip in the opposite direction before detaching from the surface.

In this paper, we present a mathematical description of the Painlevé paradox, in the presence of a compliance with both stiffness and damping, when the rigid body model has no solutions (the inconsistent case). Although we use the classical Painlevé problem as a guide, our quantitative results apply directly to a more general class of rigid body, such as the two-link manipulator [32]. Using geometric singular perturbation theory and blowup [15, 16], we solve the problem for arbitrary values of the compliance damping and give explicit

asymptotic expressions in the limiting cases of small and large damping, all for a large class of rigid body. Our approach is similar to that used in [13, 14] to understand the forward problem in piecewise smooth systems in the presence of a two-fold. In the present paper, we exploit the fact that the fast solution is unstable in the inconsistent case, by following its unstable direction until the rod sticks. Then we solve the problem both in the stick phase and in the phase where the rod lifts off the surface.

The paper is organized as follows. In Section 2, we introduce the problem, outline some of the main results known to date and include compliance. In Section 3, we give a summary of our main results, for the convenience of the reader, before presenting their derivation in Section 4. We outline our conclusions in Section 5.

## 2 Classical Painlevé problem

Consider a rigid rod  $AB$ , slipping on a rough horizontal surface, as depicted in Fig. 1.

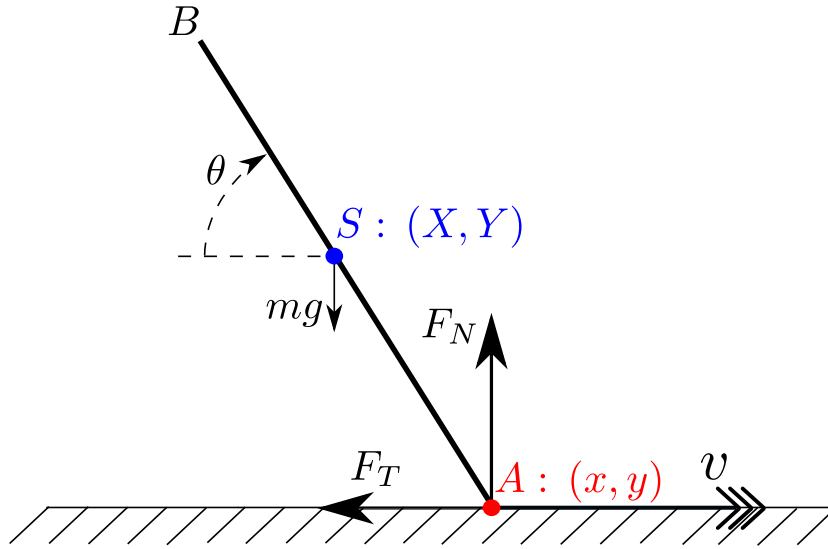


Figure 1: The classical Painlevé problem.

The rod has mass  $m$ , length  $2l$ , the moment of inertia of the rod about its center of mass  $S$  is given by  $I$  and its center of mass coincides with its center of gravity. The point  $S$  has coordinates  $(X, Y)$  relative to an inertial frame of reference  $(x, y)$  fixed in the rough surface. The rod makes an angle  $\theta$  with respect to the horizontal, with  $\theta$  increasing in a clockwise direction. At  $A$ , the rod experiences a contact force  $(F_T, F_N)$ , which opposes the motion.

The dynamics of the rod is then governed by the following equations

$$\begin{aligned} m\ddot{X} &= -F_T, \\ m\ddot{Y} &= -mg - F_N, \\ I\ddot{\theta} &= -l(\cos\theta F_N - \sin\theta F_T). \end{aligned} \quad (1)$$

where  $g$  is the acceleration due to gravity.

The coordinates  $(X, Y)$  and  $(x, y)$  are related geometrically as follows

$$\begin{aligned} x &= X + l \cos \theta, \\ y &= Y - l \sin \theta. \end{aligned} \quad (2)$$

We now adopt the scalings

$$(X, Y) = l(\tilde{X}, \tilde{Y}), \quad (x, y) = l(\tilde{x}, \tilde{y}), \quad (F_T, F_N) = mg(\tilde{F}_T, \tilde{F}_N), \quad t = \frac{1}{\omega} \tilde{t},$$

where  $\omega^2 = \frac{g}{l}$ . In addition we set  $\alpha = \frac{ml^2}{I}$ . Note that for a uniform rod,  $I = \frac{1}{3}ml^2$ , and so  $\alpha = 3$  in this case.

Then for general  $\alpha$ , (1) and (2) can be combined to become, on dropping the tildes,

$$\begin{aligned} \ddot{x} &= -\dot{\theta}^2 \cos \theta + \alpha \sin \theta \cos \theta F_N - (1 + \alpha \sin^2 \theta) F_T, \\ \ddot{y} &= -1 + \dot{\theta}^2 \sin \theta + (1 + \alpha \cos^2 \theta) F_N - \alpha \sin \theta \cos \theta F_T, \\ \ddot{\theta} &= -\alpha(\cos \theta F_N - \sin \theta F_T). \end{aligned} \quad (3)$$

To proceed, we need to determine the relationship between  $F_N$  and  $F_T$ . We assume Coulomb friction between the rod and the surface. Hence, when  $\dot{x} = v \neq 0$ , we set

$$F_T = \mu \text{sign}(\dot{x}) F_N, \quad (4)$$

where  $\mu$  is the coefficient of friction. By substituting (4) into (3), we obtain two sets of governing equations for the motion, depending on the sign of  $\dot{x}$ , which can be written as follows:

$$\begin{aligned} \dot{x} &= v, \\ \dot{y} &= a(\theta, \phi) + q_{\pm}(\theta) F_N, \\ \dot{\theta} &= \phi, \\ \dot{\phi} &= b(\theta, \phi) + p_{\pm}(\theta) F_N, \\ \dot{\phi} &= c_{\pm}(\theta) F_N, \end{aligned} \quad (5)$$

where the variables  $v, w, \phi$  denote velocities in the  $x, y, \theta$  directions respectively and

$$\begin{aligned} a(\theta, \phi) &= -\phi^2 \cos \theta, \\ b(\theta, \phi) &= -1 + \phi^2 \sin \theta, \\ q_{\pm}(\theta) &= \alpha \sin \theta \cos \theta \mp \mu(1 + \alpha \sin^2 \theta), \\ p_{\pm}(\theta) &= 1 + \alpha \cos^2 \theta \mp \mu \alpha \sin \theta \cos \theta, \\ c_{\pm}(\theta) &= -\alpha(\cos \theta \mp \mu \sin \theta) \end{aligned} \quad (6)$$

for the configuration in Fig. 1. The suffices  $q_{\pm}, p_{\pm}, c_{\pm}$  correspond to  $\dot{x} = v \geq 0$  respectively.

We will work with system (5) henceforth. Our results do not rely on the particular functions  $q_{\pm}, p_{\pm}$  and  $c_{\pm}$  in (6). We only exploit their signs and the structure of the  $\mu$ -dependency: Their sums are independent of  $\mu$  while their differences are proportional to  $\mu$ . The results therefore hold for other mechanical systems with different  $q_{\pm}, p_{\pm}$  and  $c_{\pm}$  and even dependency on several angles  $\theta \in \mathbb{T}^d$ , e.g. the two-link mechanism of Zhao *et al.* [32].

When  $\dot{x} = v = 0$  and  $\dot{v}$  for  $v \geq 0$  is opposing  $v = 0$ , then Filippov's method [8] gives us the required vector field, described by the following lemma:

**Proposition 1** *The Filippov system within the switching manifold  $\dot{x} = v = 0$  with*

$$a(\theta, \phi) + q_+(\theta)F_N < 0 < a(\theta, \phi) + q_-(\theta)F_N,$$

is given by

$$\begin{aligned} \dot{y} &= w, \\ \dot{w} &= b(\theta, \phi) + S_w(\theta)F_N, \\ \dot{\theta} &= \phi, \\ \dot{\phi} &= S_{\phi}(\theta)F_N, \end{aligned} \tag{7}$$

where

$$\begin{aligned} S_w(\theta) &= \frac{q_-(\theta)}{q_-(\theta) - q_+(\theta)}p_+(\theta) - \frac{q_+(\theta)}{q_-(\theta) - q_+(\theta)}p_-(\theta) \\ &= \frac{1 + \alpha}{1 + \alpha \sin^2 \theta}, \\ S_{\phi}(\theta) &= \frac{q_-(\theta)}{q_-(\theta) - q_+(\theta)}c_+(\theta) - \frac{q_+(\theta)}{q_-(\theta) - q_+(\theta)}c_-(\theta) \\ &= -\frac{\alpha \cos \theta}{1 + \alpha \sin^2 \theta}. \end{aligned} \tag{8} \quad \square$$

**PROOF** The Filippov vector-field is obtained from the (state dependent) linear combination of the two vector-fields  $v \geq 0$  that gives  $\dot{v} = 0$ . The system (7) is therefore obtained from a simple calculation. The explicit expressions for  $S_w$  and  $S_{\phi}$  are obtained using (6).  $\blacksquare$

**Remark 1** Note that both  $S_w$  and  $S_{\phi}$  are independent of  $\mu$ . This is true for general  $c_{\pm}, q_{\pm}$  and  $p_{\pm}$ . It is a simple consequence of the structure of their  $\mu$ -dependence.  $\square$

We will refer to the motion within  $v = 0$  described by Filippov and the equations (7) as *sticking* (rather than sliding as is common in the piecewise-smooth literature [8]). In the sequel, we consider the rod to be initially moving to the right ( $v > 0$ ), in contact with the surface ( $y = w = 0$ ), inclined at an angle  $\theta$ . We then wish to determine what happens next.

In order to solve (5) and (7), we need to determine  $F_N$ . There are two ways to proceed: the constraint-based method and the compliance-based method. The former approach leads to the Painlevé paradox. The latter approach is the subject of this paper.

## 2.1 Constraint-based method

In the constraint-based method, in order to maintain the constraint  $y = 0$ ,  $\ddot{y}$  ( $= \dot{w}$ ) and  $F_N$  form a complementarity pair given by

$$\dot{w} \geq 0, \quad F_N \geq 0, \quad F_N \cdot \dot{w} = 0. \quad (9)$$

Note that  $F_N \geq 0$  since the rough surface can only push the rod; not pull the rod.

As a consequence of (9),  $F_N$  and  $y$  satisfy the complementarity conditions

$$0 \leq F_N \perp y \geq 0. \quad (10)$$

In other words, at most one of  $F_N$  and  $y$  can be positive. For the system shown in Fig. 1, the Painlevé paradox occurs when  $v > 0$  and  $\theta \in (0, \frac{\pi}{2})$ , provided  $p_+(\theta) < 0$ , as follows.

From the fourth equation in (5), we can see that  $b$  is the free acceleration of the end of the rod. Therefore if  $b > 0$ , lift-off is always possible when  $y = w = 0$ . But if  $b < 0$ , in equilibrium we would expect a forcing term  $F_N$  to maintain the rod on  $y = 0$ . From  $\dot{w} = 0$  we obtain

$$F_N = -\frac{b}{p_+} \quad (11)$$

since  $v > 0$ . But since  $F_N \geq 0$ , this requires  $p_+ > 0$ . From (6), it can be seen that this is always true for  $\theta \in (\frac{\pi}{2}, \pi)$ .

But if  $p_+ < 0$ , then the expression for  $F_N$  in (11) is negative. Then  $F_N$  is in an *inconsistent* (or *non-existent*) mode. This can happen, provided  $\theta \in (0, \frac{\pi}{2})$ .

Note that if  $b > 0$  and  $p_+ < 0$  then lift-off is always possible from  $y = 0$ . But at the same time  $F_N$  in (11) is positive. Then  $F_N$  is in an *indeterminate* (or *non-unique*) mode.

We focus on the inconsistent case. It is straightforward to show that  $p_+(\theta) < 0$  requires

$$\mu > \mu_c(\alpha) \equiv \frac{2}{\alpha} \sqrt{1 + \alpha}. \quad (12)$$

Then the Painlevé paradox can occur for  $\theta \in (\theta_1, \theta_2)$  where

$$\begin{aligned} \theta_1(\mu, \alpha) &= \arctan \frac{1}{2} \left( \mu\alpha - \sqrt{\mu^2\alpha^2 - 4(1 + \alpha)} \right), \\ \theta_2(\mu, \alpha) &= \arctan \frac{1}{2} \left( \mu\alpha + \sqrt{\mu^2\alpha^2 - 4(1 + \alpha)} \right). \end{aligned} \quad (13)$$

For a uniform rod with  $\alpha = 3$ , we have  $\mu_c = \frac{4}{3}$ . For  $\alpha = 3$  and  $\mu = 1.4$  the dynamics can be summarized in the  $(\theta, \phi)$ -plane, as in Fig. 2 (compare with Figure 2 of Génot and Brogliato [9], where the authors plot the unscaled angular velocity  $\omega\phi$  vs.  $\theta$  where  $\omega = \sqrt{\frac{g}{l}}$ , for the case  $g = 9.8 \text{ ms}^{-2}$ ,  $l = 1 \text{ m}$ ).

Along  $\theta = \theta_1, \theta_2$ , we have  $p_+(\theta) = 0$ . These lines intersect the curve  $b(\theta, \phi) = 0$  at four points:  $\phi_{1,2}^\pm = \pm \sqrt{\text{csc} \theta_{1,2}}$ . Génot and Brogliato [9] showed that the point  $P : (\theta, \phi) = (\theta_1, \sqrt{\text{csc} \theta_1})$  is the most important and analyzed the local dynamics around it. In the first quadrant centered on  $P$  (colored violet in Fig. 2), we have  $b > 0$ ,  $p_+ < 0$ , so the dynamics is indeterminate (non-unique). In the second quadrant (colored orange in Fig. 2),  $b > 0$ ,  $p_+ >$

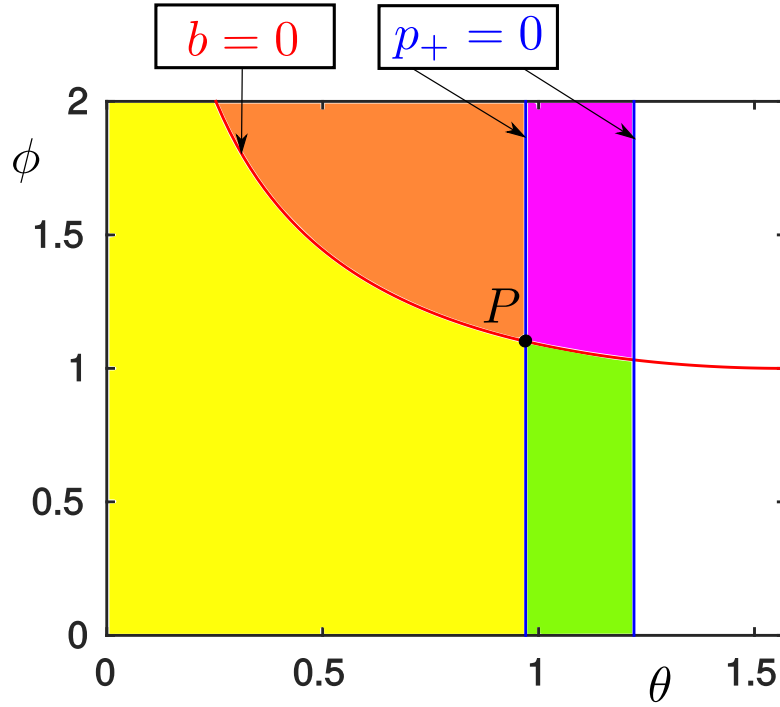


Figure 2: The  $(\theta, \phi)$ -plane for the classical Painlevé problem of Fig. 1, for  $\alpha = 3$  and  $\mu = 1.4$ . The point  $P$  has coordinates  $(\theta_1, \sqrt{\csc \theta_1})$ , where  $\theta_1$  is given in (13).

0 and the rod lifts off the rough surface. In the third quadrant (colored yellow in Fig. 2),  $b < 0$ ,  $p_+ > 0$  and the rod moves (slips) along the surface. Génot and Brogliato [9] showed that the dynamics here cannot cross  $p_+ = 0$  unless also  $b = 0$ . In the fourth quadrant (colored green in Fig. 2),  $b < 0$ ,  $p_+ < 0$  and the dynamics is inconsistent; there exists no positive value of  $F_N$ , even though the constraint  $y = 0$  is satisfied, in contradiction of the complementarity conditions (10).

The behaviour in this fourth quadrant is the focus of this paper. The third quadrant, and the role of  $P$  under regularization, will be the subject of a separate paper. The rigid body equations (1) that we have adopted so far are unable to resolve the dynamics in the fourth quadrant. So we must regularize (1) by relaxing some of the (implicit) assumptions used to derive these equations.

## 2.2 Compliance-based method

To proceed, we assume that there is compliance at the point  $A$  between the rod and the surface, when they are in contact. In particular, following [7, 20], we assume that there are small excursions into  $y < 0$ . Then we require that the normal force  $F_N = F_N(y, w)$  and that  $\partial_y F_N < 0$ ,  $\partial_w F_N < 0$ . Our analysis can handle any such form of  $F_N$  (see Remark 6 below). But, for our quantitative results, we take the (scaled) normal reaction  $F_N$  to be a function

of  $(y, w)$  of the form

$$F_N(y, w) = \begin{cases} 0 & \text{for } y > 0 \\ \max\{-ky - \gamma w, 0\} & \text{for } y \leq 0, \end{cases} \quad (14)$$

where  $k, \gamma$  are both positive and represent a (scaled) spring constant and damping coefficient, respectively. We are interested in the case when the compliance is very large, so introduce a small parameter  $\epsilon$  as follows:

$$k = \epsilon^{-2}, \quad \gamma = \epsilon^{-1}\delta. \quad (15)$$

This choice of scaling was used by McClamroch [20] and Dupont and Yamajako [7]. It ensures that the critical damping coefficient is independent of  $\epsilon$ . In fact  $\delta_{crit} = 2$ .

In what follows, the first equation in (5) will play no role, so we drop it from now on. Thus we combine the remaining five equations in (5) with (14) and (15) to give the set of governing equations that we will use in the sequel

$$\begin{aligned} \dot{y} &= w, \\ \dot{w} &= b(\theta, \phi) + p_{\pm}(\theta)[- \epsilon^{-2}y - \epsilon^{-1}\delta w], \\ \dot{\theta} &= \phi, \\ \dot{\phi} &= c_{\pm}(\theta)[- \epsilon^{-2}y - \epsilon^{-1}\delta w], \\ \dot{v} &= a(\theta, \phi) + q_{\pm}(\theta)[- \epsilon^{-2}y - \epsilon^{-1}\delta w], \end{aligned} \quad (16)$$

where we interpret the quantity in square brackets as vanishing when the argument  $\epsilon^{-2}y + \epsilon^{-1}\delta w > 0$  or  $y > 0$  cf. (14).

The compliant Filippov system is obtained from (7) by replacing  $F_N$  with the square bracket  $[-\epsilon^{-2}y - \epsilon^{-1}\delta w]$ .

**Remark 2** It is easy to show that the energy of the system

$$E = \frac{1}{2}(\dot{X}^2 + \dot{Y}^2) + \frac{1}{2}\frac{\phi^2}{\alpha} + gY + \frac{1}{2}\frac{y^2}{\epsilon^2},$$

is non-increasing:

$$\dot{E} = -\mu|v|F_N(y, w) - \frac{\delta}{\epsilon}w^2 \leq 0,$$

as expected. □

### 3 Main Results

In this section we present the main result of the paper, Theorem 1 below. We will recover IWC, when the rigid body moves to the right  $v > 0$  in an inconsistent state, by calculating the vertical velocity  $w$  in terms of the initial horizontal velocity  $v_0 > 0$ , after an excursion into  $y < 0$ , that occurs instantaneously as  $\epsilon \rightarrow 0$ . We solve the problem for arbitrary values of the compliance damping  $\delta$  and give explicit asymptotic expressions for  $\delta \gg 1$  and  $\delta \ll 1$  for a large class of rigid body.



**Theorem 1** Consider an initial condition

$$(y, w, \theta, \phi, v) = (0, 0, \theta_0, \phi_0, v_0), \quad v_0 > 0, \quad (17)$$

within the region of inconsistency (non-existence) where

$$p_+(\theta_0) < 0, \quad b(\theta_0, \phi_0) < 0, \quad (18)$$

and  $q_+(\theta_0) < 0$ ,  $q_-(\theta_0) > 0$ ,  $a(\theta_0) \neq 0$ . Then the forward flow of (17) under (16) returns to  $\{(y, w, \theta, \phi, v) | y = 0\}$  after a time  $\mathcal{O}(\epsilon \ln \epsilon^{-1})$  with

$$\begin{aligned} w &= e(\delta, \theta_0)v_0 + o(1), \\ \theta &= \theta_0 + o(1), \\ \phi &= \phi_0 + \left\{ -\frac{c_+(\theta_0)}{q_+(\theta_0)} + \frac{S_\phi(\theta_0)}{S_w(\theta_0)} \left( e(\delta, \theta_0) + \frac{p_+(\theta_0)}{q_+(\theta_0)} \right) \right\} v_0 + o(1), \\ v &= o(1), \end{aligned}$$

as  $\epsilon \rightarrow 0$ . During this period  $y = \mathcal{O}(\epsilon)$ ,  $w = \mathcal{O}(1)$  so that  $F_N = \mathcal{O}(\epsilon^{-1})$ . The function  $e(\delta, \theta_0)$  is smooth and has the following asymptotic expansions:

$$\begin{aligned} e(\delta, \theta_0) &= \frac{p_-(\theta_0) - p_+(\theta_0)}{q_-(\theta_0)p_+(\theta_0) - q_+(\theta_0)p_-(\theta_0)} \delta^{-2} (1 + \mathcal{O}(\delta^{-2} \ln \delta^{-4})) \quad \text{for } \delta \gg 1, \\ e(\delta, \theta_0) &= \sqrt{\frac{p_+(\theta_0)(p_-(\theta_0) - p_+(\theta_0))}{q_+(\theta_0)(q_-(\theta_0) - q_+(\theta_0))}} \left( 1 - \frac{\sqrt{S_w(\theta_0)}}{2} \left( \pi - \arctan \left( \sqrt{-\frac{S_w(\theta_0)}{p_+(\theta_0)}} \right) \right) \delta + \mathcal{O}(\delta^2) \right) \quad \text{for } \delta \ll 1. \quad \square \end{aligned}$$

**Remark 3** The general expression for  $e(\delta, \theta_0)$  is given in (45) below. Plots of  $e(\delta, \theta_0)$  for  $q_\pm$  and  $p_\pm$  in (6) indicate that it is monotonically decreasing:

$$\partial_\delta e(\delta, \theta_0) < 0,$$

for every  $\theta_0 \in (\theta_1, \theta_2)$  in the inconsistent state. □

**Remark 4** The leading order expression for  $e(\delta, \theta_0)$  for  $\delta \gg 1$  is independent of  $\mu$ , in general. Using the expressions for  $q_\pm$  and  $p_\pm$  in (6), we find for large  $\delta$  that

$$e(\delta, \theta_0) = \frac{\alpha}{2(1+\alpha)} \sin(2\theta_0) \delta^{-2} (1 + \mathcal{O}(\delta^{-2} \ln \delta^{-4})), \quad \theta_0 \in (\theta_1, \theta_2). \quad (19)$$

The limit  $\delta \rightarrow \infty$  is not uniform in  $\theta \in (\theta_1, \theta_2)$ . Furthermore, the leading order coefficient  $\frac{\alpha}{2(1+\alpha)} \sin(2\theta_0)$  is generally not monotonic in  $\theta_0 \in (\theta_1, \theta_2)$ , since  $\theta_1$  can be either less or greater than  $\pi/4$ . However, for  $\alpha = 3$  and  $\mu = 1.4$  we have  $\theta_1 > \frac{\pi}{4}$  and hence  $e(\delta, \theta_0)$  is monotonically decreasing as a function of  $\theta_0$  for  $\delta \gg 1$  in this case.

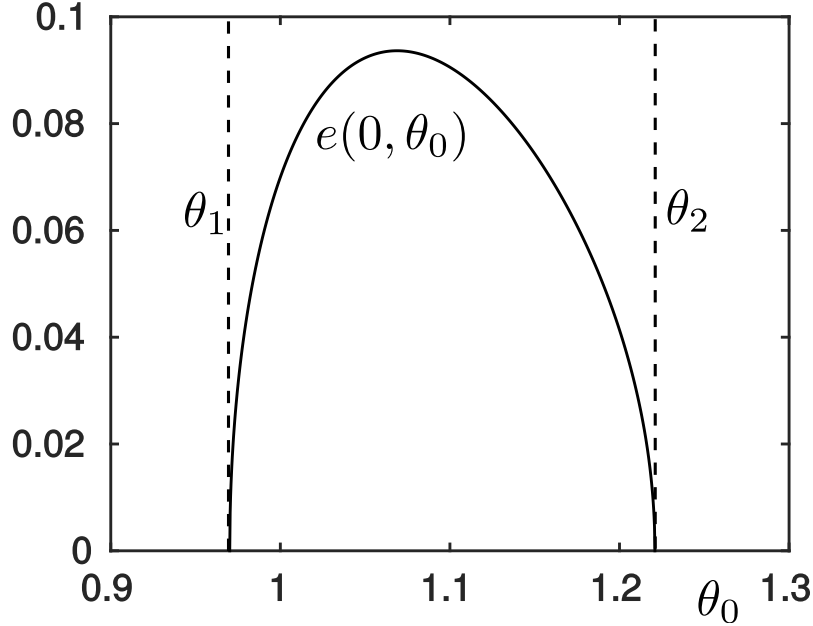


Figure 3: Plot of  $e(0, \theta_0)$  for  $\alpha = 3$  and  $\mu = 1.4$ .

The expression for  $\delta \ll 1$  is more complicated and *does* depend upon  $\mu$ , in general. Using the expressions for  $q_{\pm}$  and  $p_{\pm}$  in (6), for  $\delta = 0$  we have:

$$e(0, \theta_0) = \sqrt{\frac{(1 + \alpha \cos^2 \theta_0 - \mu \alpha \sin \theta_0 \cos \theta_0)}{(\alpha \sin \theta_0 \cos \theta_0 - \mu(1 + \alpha \sin^2 \theta_0))} \frac{\alpha \sin \theta \cos \theta_0}{(1 + \alpha \sin^2 \theta_0)}}$$

We plot  $e(0, \theta_0)$  in Fig. 3 for  $\alpha = 3$  and  $\mu = 1.4$ . □

We will prove Theorem 1 in the following section using geometric singular perturbation theory and blowup [15, 16].

## 4 Proof of Theorem 1

The proof of Theorem 1 will be divided into three phases, illustrated in Fig. 4.

- Slipping compression (section 4.2): During this period  $y$ ,  $w$  and  $v$  all decrease. Geometrically, we find that the dynamics follow an unstable manifold  $\gamma^u$  of a set of critical points  $C$  as  $\epsilon \rightarrow 0$ . Along  $\gamma^u$  the normal force  $F_N(y, w)$  increases. We will show that  $F_N = \mathcal{O}(\epsilon^{-1})$  and  $v$  will therefore quickly decrease to 0. Mathematically this part is complicated by the fact that the initial condition (17) belongs to the critical set  $C$  as  $\epsilon \rightarrow 0$ . We therefore apply a blowup of  $C$  (see Section 4.2.1) which enables us to guide the initial condition close to  $C$  along  $\gamma^u$ .

- Sticking (section 4.3): Since  $F_N = \mathcal{O}(\epsilon^{-1})$  and  $q_+q_- < 0$  the rod will in the next phase stick with  $v \equiv 0$ . During this period  $\dot{y} = \dot{w} > 0$  and eventually sticking ceases with  $F_N = 0$  as  $\epsilon \rightarrow 0$ .
- Lift off (section 4.4): In the final phase  $F_N = 0$  and lift off occurs.

In [32], the sticking phase is further divided into two parts: “sticking compression” and “sticking restitution”. A similar sub-division is possible using our compliance-based approach, corresponding to  $\dot{w} < 0$  and  $\dot{w} > 0$ , respectively. But mathematically these phases are described by the same set of equations.

In the following section 4.1, we first describe the slow-fast setting.

#### 4.1 Slow-fast setting: Initial scaling

To study (16) we first apply the following scaling:

$$y = \epsilon \hat{y},$$

which brings the terms in

$$F_N(y, w) = [-\epsilon^{-2}y - \epsilon^{-1}\delta w] = \epsilon^{-1}[-\hat{y} - \delta w], \quad (20)$$

to the same order. This scaling was also used in [20]. Let

$$\hat{F}_N(\hat{y}, w) \equiv F_N(\epsilon \hat{y}, w).$$

The equations with  $v > 0$  then read:

$$\begin{aligned} \hat{y}' &= w, \\ w' &= \epsilon b(\theta, \phi) + p_+(\theta) [-\hat{y} - \delta w], \\ \theta' &= \epsilon \phi, \\ \phi' &= c_+(\theta) [-\hat{y} - \delta w], \\ v' &= \epsilon a(\theta, \phi) + q_+(\theta) [-\hat{y} - \delta w], \end{aligned} \quad (21)$$

with respect to the fast time

$$\tau = \epsilon^{-1}t : \quad ()' = \frac{d}{d\tau}.$$

This is slow-fast system in non-standard form. Only  $\theta$  is truly slow whereas  $(\hat{y}, w, \phi, v)$  are all fast. But the set of critical points

$$C = \{(\hat{y}, w, \theta, \phi, v) | \hat{y} = w = 0\}, \quad (22)$$

for  $\epsilon = 0$  is just three dimensional.

**Proposition 2**  $C$  is normally hyperbolic for  $p_+(\theta) \neq 0$ . In particular, it is of saddle-type for  $p_+(\theta) < 0$ . The unstable manifold  $\gamma^u(\theta_0, \phi_0, v_0)$  of  $(\hat{y}, w, \theta, \phi, v) = (0, 0, \theta_0, \phi_0, v_0) \in C$  contained within  $\hat{F}_N \geq 0$  is given by

$$\begin{aligned} \gamma^u(\theta_0, \phi_0, v_0) : \quad w &= \lambda_+ \hat{y}, \\ \theta &= \theta_0, \\ \phi &= \phi_0 + \frac{c_+(\theta_0)}{p_+(\theta_0)} \lambda_+(\theta_0) \hat{y}, \\ v &= v_0 + \frac{q_+(\theta_0)}{p_+(\theta_0)} \lambda_+(\theta_0) \hat{y}, \\ \hat{y} &\leq 0, \end{aligned} \tag{23}$$

with  $\lambda_+(\theta_0) > 0$  as in (24) below.  $\square$

PROOF  $C$  is clearly a set of critical points for  $\epsilon = 0$ . The linearization about a point in  $C$  gives one single  $2 \times 2$  block

$$\begin{pmatrix} 0 & 1 \\ -p_+(\theta) & -\delta p_+(\theta) \end{pmatrix},$$

with non-zero eigenvalues:

$$\lambda_{\pm}(\theta) = -\frac{\delta p_+(\theta)}{2} \pm \frac{1}{2} \sqrt{\delta^2 p_+(\theta)^2 - 4p_+(\theta)}, \tag{24}$$

satisfying

$$\lambda_{\pm}^2 = -p_+(\theta) (1 + \delta \lambda_{\pm}). \tag{25}$$

For  $p_+(\theta) < 0$  the eigenvalues satisfy  $\lambda_- < 0 < \lambda_+$ . The eigenvector associated with  $\lambda_+$  is

$$\begin{aligned} v_+ &= (1, \lambda_+, -c_+ \lambda_+^{-1} (1 + \delta \lambda_+), -q_+ \lambda_+^{-1} (1 + \delta \lambda_+)) \\ &= \left( 1, \lambda_+, \frac{c_+}{p_+} \lambda_+, \frac{q_+}{p_+} \lambda_+ \right), \end{aligned}$$

using (25).  $\blacksquare$

**Remark 5** The saddle structure of  $C$  within the inconsistency region has been recognized by many authors [1, 7, 27].  $\square$

**Remark 6** Our arguments below are geometrical and rely only on hyperbolic methods of dynamical systems theory. Qualitatively the results therefore remain unchanged if we replace the linear  $\hat{F}_N$  in (20) with a nonlinear version

$$\hat{F}_N(\hat{y}, w) = \epsilon^{-1} [-\hat{y} - \delta w + \mathcal{O}((\hat{y} + w)^2)], \tag{26}$$

having (20) as its linearization about  $\hat{y} = w = 0$ . Then we would again obtain a saddle-type critical set  $C$  with (nonlinear) unstable manifold  $\gamma^u$ .  $\square$

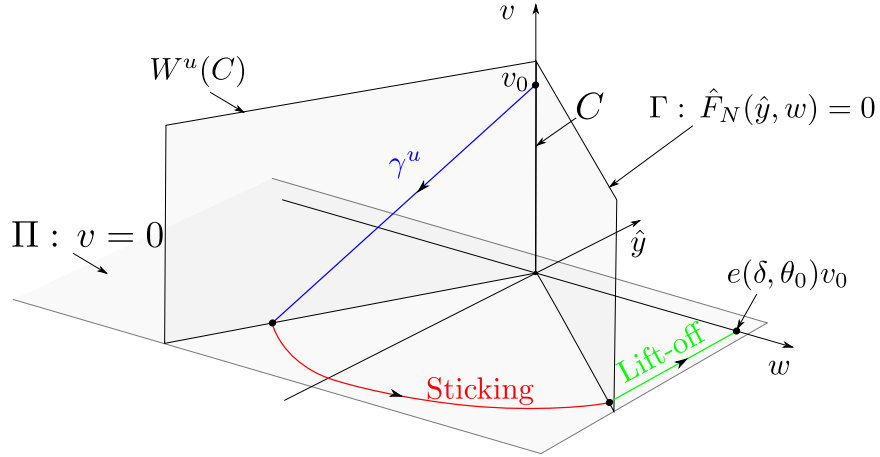


Figure 4: The limit  $\epsilon \rightarrow 0$  is described by three phases. The first phase of slipping compression, where  $\hat{y}$ ,  $w$  and  $v > 0$  all decrease, is described geometrically by an unstable manifold  $\gamma^u$  (23) (in blue) of a critical set  $C$  in (22). The next phase of sticking (in red) is described by Filippov. Here  $\hat{y}'' = w' > 0$  and eventually sticking ceases with  $F_N = 0$ . Finally lift-off (in green) occurs and we return to  $\hat{y} = 0$ . Mathematically, the main challenge of the problem is within the initial phase and is due to the fact that the initial condition (17) belongs to the critical set  $C$  as  $\epsilon \rightarrow 0$ . We therefore apply a blowup of  $C$  (see Section 4.2.1 and Fig. 5). This enables us to guide the initial condition close to  $C$  along  $\gamma^u$ .

## 4.2 Slipping compression

In this section we will describe the first phase for the IWC: *slipping compression*. This period will end when  $v = 0$ . We therefore define the following section

$$\Pi = \{(\hat{y}, w, \theta, \phi, v) | v = 0\}. \quad (27)$$

The main result of this section is Proposition 3. It describes the intersection of the forward flow of the initial conditions (17) (or (28) below) with  $\Pi$ . In other words, it gives the values of  $\hat{y}, w, \theta, \phi$ , given in (29), at the end of the slipping compression phase. Then, in section 4.3, we will use these values to initialize the next phase, which we know from Lemma 1 below, is a stick phase.

**Proposition 3** *The forward flow of the initial conditions*

$$(\hat{y}, w, \theta, \phi, v) = (0, 0, \theta_0, \phi_0, v_0), \quad v_0 > 0, \quad (28)$$

under (21) intersects  $\Pi$  with

$$\begin{aligned}\hat{y} &= -\frac{p_+(\theta_0)}{q_+(\theta_0)\lambda_+(\theta_0)}v_0 + \mathcal{O}(\epsilon^c), \\ w &= -\frac{p_+(\theta_0)}{q_+(\theta_0)}v_0 + \mathcal{O}(\epsilon^c), \\ \theta &= \theta_0 + \mathcal{O}(\epsilon^c), \\ \phi &= \phi_0 - \frac{c_+(\theta_0)}{q_+(\theta_0)}v_0 + \mathcal{O}(\epsilon^c),\end{aligned}\tag{29}$$

for  $c \in (0, 1)$  sufficiently small, as  $\epsilon \rightarrow 0$ . □

**Remark 7** Note that (29) is  $o(1)$ -close to the unstable manifold in (23). □

In addition we have

**Lemma 1** At (29) within  $\Pi : v = 0$  the motion sticks for  $\epsilon \ll 1$  and is therefore described by (7). □

PROOF This follows from the fact that  $\hat{F}_N > 0$  and  $q_+q_- < 0$ . ■

We prove Proposition 3 as follows. In the scaling of (21) the initial conditions (17) belong to  $C$  for  $\epsilon = 0$ . To proceed we will have to employ the following subsequent zoom (scaling)

$$\kappa_1 : \quad \hat{y} = r_1\hat{y}_1, \quad w = r_1w_1, \quad \epsilon = r_1,\tag{30}$$

focussing in on  $\hat{y} = w = \epsilon = 0$ .

**Remark 8** In terms of the original variables we have  $y = \epsilon^2\hat{y}_1$ ,  $w = \epsilon w_1$ . The variables  $(\hat{y}_1, w_1)$  were also used in [5], where they were denoted by  $(\tilde{y}, \tilde{v})$ . □

The scaling  $\kappa_1$  in (30) gives rise to the following equations:

$$\begin{aligned}\hat{y}'_1 &= w_1, \\ w'_1 &= b(\theta, \phi) + p_+(\theta) [-\hat{y}_1 - \delta w_1], \\ \theta' &= \epsilon\phi, \\ \phi' &= \epsilon c_+(\theta) [-\hat{y}_1 - \delta w_1], \\ v' &= \epsilon (a(\theta, \phi) + q_+(\theta) [-\hat{y}_1 - \delta w_1]),\end{aligned}\tag{31}$$

**Remark 9** If we replace the linear  $\hat{F}_N$  with a nonlinear version (26) having (20) as the linearization about  $\hat{y} = w = 0$  then the square bracket in (31) becomes

$$[-\hat{y}_1 - \delta w_1 + \mathcal{O}(\epsilon)],$$

and the  $\epsilon = 0$  limiting system is therefore independent of these nonlinear terms. □

Equation (31) is a slow-fast system in standard form:  $(\hat{y}_1, w_1)$  are fast variables whereas  $(\theta, \phi, v)$  are slow variables. Since the square bracket  $[-\hat{y}_1 - \delta w_1]$  vanishes for  $\hat{y}_1 > 0$  (recall the definition of the square bracket below (16)) there exists no critical set for  $(31)_{\epsilon=0}$ . The set

$$C_1 = \{(\hat{y}_1, w_1, \theta, \phi, v) | \hat{y}_1 = \frac{b(\theta, \phi)}{p_+(\theta)}, w_1 = 0\},$$

is by assumption of  $b < 0, p_+ < 0$  contained within  $\hat{y}_1 > 0$ . However, if we retain  $[-\hat{y}_1 - \delta w_1]$  in (31) for  $\hat{y}_1 > 0$ , then  $C_1$  (as  $C$ ) is of saddle type. The unstable manifold of  $C_1$  with base point

$$(\hat{y}_1, w_1, \theta, \phi, v) = \left( \frac{b(\theta_0, \phi_0)}{p_+(\theta_0)}, 0, \theta_0, \phi_0, v_0 \right),$$

contained within  $\hat{y}_1 \leq 0$  will play an important role in the following. It is given as

$$\begin{aligned} \gamma_1^u(\theta_0, \phi_0, v_0) : \quad & \hat{y}_1 = \frac{b(\theta_0, \phi_0)}{p_+(\theta_0)} + s, \\ & w_1 = \lambda_+(\theta_0)s, \\ & \theta = \theta_0, \\ & \phi = \phi_0, \\ & v = v_0, \\ & s \leq -\frac{b(\theta_0, \phi_0)}{p_+(\theta_0)}. \end{aligned}$$

Note that  $C_1$  upon returning to  $(\hat{y}, w)$  through (30) gives  $C$  in (22) upon setting  $\epsilon = 0$ . It is clear that our initial condition

$$(\hat{y}_1, w_1, \theta, \phi, v) = (0, 0, \theta_0, \phi_0, v_0),$$

by the linearity and the saddle structure of  $C_1$  will contract towards the unstable manifold  $\gamma_1^u$  as  $\hat{y}_1, w_1 \rightarrow -\infty$ . But for  $\epsilon > 0$  the variables  $(\phi, v)$  will start to vary by  $\mathcal{O}(1)$ -amount as  $\hat{y}_1, w_1 \rightarrow -\infty$ . The variables  $(\phi, v)$  are slow in (31) but fast in (21). We will therefore need to do some matching between the two systems.

#### 4.2.1 Blowup of $C$

One nice general way of achieving the matching of (31) and (21) geometrically is to view the scaling in (30) as part of the following blowup transformation  $(r, \bar{y}, \bar{w}, \bar{\epsilon}) \mapsto (\hat{y}, w, \epsilon)$  given by:

$$\hat{y} = r\bar{y}, \quad w = r\bar{w}, \quad \epsilon = r\bar{\epsilon}, \quad r \geq 0, \quad (\bar{y}, \bar{w}, \bar{\epsilon}) \in S^2 = \{(x, y, z) | x^2 + y^2 + z^2 = 1\}. \quad (32)$$

This transformation blows up each point in  $C = \{(\hat{y}, w, \theta, \phi, v) | \hat{y} = w = 0\}$  to a sphere  $S^2$  for  $r = 0$ . In the blowup variables

$$(r, (\bar{y}, \bar{w}, \bar{\epsilon}), \theta, \phi, v) \in \mathcal{B} \equiv \bar{\mathbb{R}}_+ \times S^2 \times S^1 \times \mathbb{R} \times \mathbb{R}_+,$$

the critical set therefore becomes a cylinder of spheres:

$$\overline{C} = \{(r, (\bar{y}, \bar{w}, \bar{\epsilon}), \theta, \phi, v) \in \mathcal{B} | r = 0\}.$$

See [15, 16] for further details of the blowup method.

The scaling  $\kappa_1$  in (30) then becomes a *scaling* chart obtained by setting  $\bar{\epsilon} = 1$  in (32) such that

$$r = r_1 \sqrt{1 + \hat{y}_1^2 + w_1^2}, \quad \bar{y} = \hat{y}_1 / \sqrt{1 + \hat{y}_1^2 + w_1^2}, \quad \bar{w} = w_1 / \sqrt{1 + \hat{y}_1^2 + w_1^2}, \quad \bar{\epsilon} = 1 / \sqrt{1 + \hat{y}_1^2 + w_1^2},$$

with

$$\bar{y}^2 + \bar{w}^2 + \bar{\epsilon}^2 = 1.$$

We will use the *directional* chart

$$\kappa_2 : \quad y = -r_2, \quad w = r_2 w_2, \quad \epsilon = r_2 \epsilon_2, \quad (33)$$

obtained by setting  $\bar{y} = -1$  in (32) to describe the part of the sphere  $(\bar{y}, \bar{w}, \bar{\epsilon}) \in S^2$  with  $\bar{y} < 0$ :

$$r = r_2 \sqrt{1 + w_2^2 + \epsilon_2^2}, \quad \bar{y} = -1 / \sqrt{1 + w_2^2 + \epsilon_2^2}, \quad \bar{w} = w_2 / \sqrt{1 + w_2^2 + \epsilon_2^2}, \quad \bar{\epsilon} = \epsilon_2 / \sqrt{1 + w_2^2 + \epsilon_2^2}.$$

For  $y_1 < 0$  we have the following coordinate change

$$\kappa_{21} : \quad r_2 = -r_1 y_1, \quad w_2 = -w_1 y_1^{-1}, \quad \epsilon_2 = -y_1^{-1}, \quad (34)$$

between the charts  $\kappa_1$  and  $\kappa_2$ . The chart  $\kappa_2$  enables a matching of  $\kappa_1 \cap \{\hat{y}_1 < 0\}$ , which will be visible within  $r_2 = 0$ , and the system (21), visible within  $\epsilon_2 = 0$ . We analyse each of the charts in the following.

We illustrate the blowup of  $C$  in Fig. 5 using a projection onto the  $(\hat{y}, w, v)$ -space. Here we have inserted the sphere  $\overline{C} \cap \{v = v_0\}$  that occurs as a result of blowing up  $C \cap \{v = v_0\}$  by (32). In Fig. 5 we also illustrate the results of the blowup analysis. Using chart  $\kappa_2$  we connect the orbit in chart  $\kappa_1$  (yellow) with the unstable manifold  $\gamma^u$  (blue) of (23).

#### 4.2.2 Chart $\kappa_1$

We can solve the equations in  $\kappa_1$  for  $\epsilon = 0$  with initial conditions  $\hat{y}_1(0) = w_1(0) = 0$ ,  $\theta(0) = \theta_0$ ,  $\phi(0) = \phi_0$ ,  $v(0) = v_0$  corresponding to (28). We obtain

$$\begin{aligned} \hat{y}_1(\tau) &= \frac{b(\theta_0, \phi_0)}{p_+(\theta_0)} + k_+ e^{\lambda_+ \tau} + k_- e^{\lambda_- \tau}, \\ w_1(\tau) &= k_+ \lambda_+ e^{\lambda_+ \tau} + k_- \lambda_- e^{\lambda_- \tau}, \end{aligned} \quad (35)$$

and  $\theta(\tau) = \theta_0$ ,  $\phi(\tau) = \phi_0$ ,  $v(\tau) = v_0$ , with

$$\begin{aligned} k_+ &= \frac{\lambda_- b(\theta_0, \phi_0)}{(\lambda_+ - \lambda_-) p_+(\theta_0)} < 0, \\ k_- &= -\frac{\lambda_+ b(\theta_0, \phi_0)}{(\lambda_+ - \lambda_-) p_+(\theta_0)} < 0, \end{aligned}$$



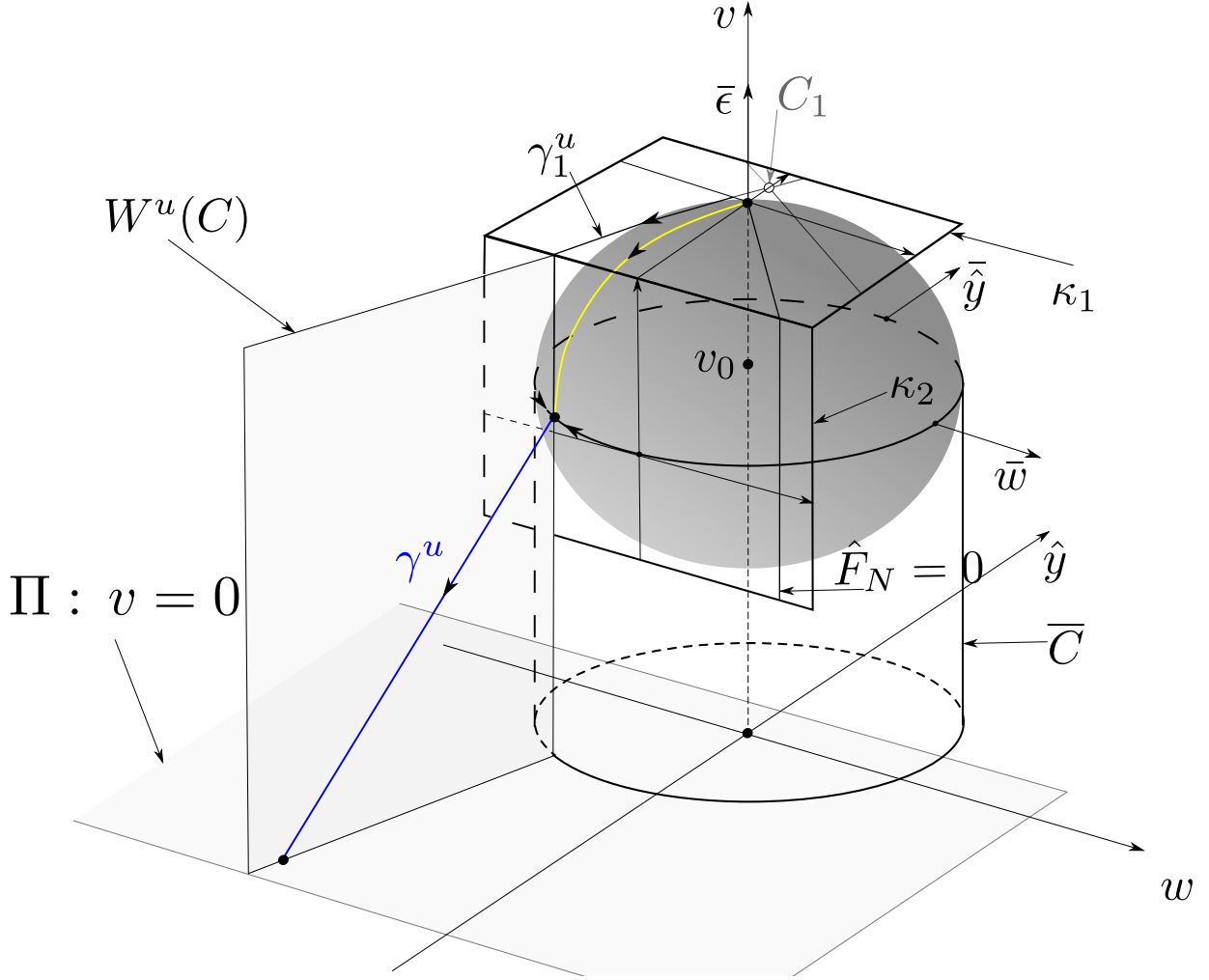


Figure 5: Illustration of the blowup  $\bar{C}$  of  $C$  by (32) using a projection onto the  $(\hat{y}, w, v)$ -space. We have inserted the sphere that occurs as a result of blowing up  $C \cap \{v = v_0\}$ . The blowup, in particular the chart  $\kappa_2$ , allows us to match the *small* (yellow), described by the chart  $\kappa_1$ , with the *large*, described by (21), and  $\gamma^u$  (blue).

by (18), and  $\lambda_{\pm}$  as in (24). Note that  $\hat{y}_1, w_1 \rightarrow -\infty$  as  $t \rightarrow \infty$ . To describe this limit we move to chart  $\kappa_1$  which covers  $\bar{y} < 0$  of the blowup sphere. Let therefore  $\nu$  be small and consider the section

$$\Lambda_1 = \{(\hat{y}_1, w_1, \theta, \phi, v) | \hat{y}_1 = -\nu^{-1}\}.$$

Clearly there exists a time  $\tau_* = \tau_*(\nu) > 0$  such that the solution for  $\epsilon = 0$  in (35) intersects  $\Lambda_1$ . Denote the intersection by  $z_1(0)$ . Then

$$z_1(0) = (-\nu^{-1}, w_{1*}, \theta_0, \phi_0, v_0),$$

where

$$w_{1*}(\nu) \equiv w_1(\tau_*) = c_+ \lambda_+ e^{\lambda_+ \tau_*} + c_- \lambda_- e^{\lambda_- \tau_*} < 0.$$

We easily obtain the following asymptotics for  $w_{1*}$ :

$$w_{1*}(\nu) = -\lambda_+ \nu^{-1} (1 + o(1)), \quad (36)$$

for  $\nu \rightarrow 0$  using that  $\lambda_- < 0 < \lambda_+$ .

For  $\epsilon \ll 1$  we therefore have by, regular perturbation theory, that the forward flow of the initial condition

$$(\hat{y}_1, w_1, \theta, \phi, v) = (0, 0, \theta_0, \phi_0, v_0),$$

intersects  $\Lambda_1$  in

$$z_1(\epsilon) = z_1(0) + \mathcal{O}(\epsilon) = (\nu^{-1}, w_{1*}(\nu) + \mathcal{O}(\epsilon), \theta_0 + \mathcal{O}(\epsilon), \phi_0 + \mathcal{O}(\epsilon), v_0 + \mathcal{O}(\epsilon)). \quad (37)$$

$z_1(\epsilon)$  is smooth in  $\epsilon$ .

### 4.2.3 Chart $\kappa_2$

Substituting (33) into (21) gives

$$\begin{aligned} \epsilon_2' &= \epsilon_2 w_2, \\ w_2' &= \epsilon_2 b(\theta, \phi) + p_+(\theta) [1 - \delta w_2] + w_2^2, \\ \theta' &= \epsilon \phi, \\ \phi' &= c_+(\theta) r_2 [1 - \delta w_2], \\ v' &= \epsilon a(\theta, \phi) + q_+(\theta) r_2 [1 - \delta w_2], \\ r_2' &= -r_2 w_2. \end{aligned} \quad (38)$$

Fix  $\rho$  small and consider the set

$$U_2 = \{(\epsilon_2, w_2, \theta, \phi, v, r_2) \mid w_2 \in [-\lambda_+ - \rho, -\lambda_+ + \rho], \epsilon_2 \in [0, \nu], r_2 \in [0, \nu]\}.$$

Then we have

**Lemma 2** *The set*

$$M_2 = \{(\epsilon_2, w_2, \theta, \phi, v, r_2) \in U_2 \mid r_2 = \epsilon_2 = 0, w_2 = -\lambda_+\},$$

*is a set of critical points of (38). The linearization gives three non-zero eigenvalues*

$$-\lambda_+ < 0, \lambda_- - \lambda_+ < 0, \lambda_+ > 0,$$

*and  $M_2$  is therefore of saddle-type. The stable manifold is*

$$W^s(M_2) = \{(\epsilon_2, w_2, \theta, \phi, v, r_2) \in U_2 \mid r_2 = 0\},$$

while the unstable manifold is

$$W^u(M_2) = \{(\epsilon_2, w_2, \theta, \phi, v, r_2) \in U_2 \mid \epsilon_2 = 0, w_2 = -\lambda_+\}.$$

In particular, the 1D unstable manifold  $\gamma_2^u(\theta_0, \phi_0, v_0) \subset W^u(M_2)$  of the base point  $(\epsilon_2, w_2, \theta, \phi, v, r_2) = (0, 0, \theta_0, \phi_0, v_0, 0)$  is given by

$$\begin{aligned} \gamma_2^u(\theta_0, \phi_0, v_0) : \quad & \theta = \theta_0, \\ & \phi = \phi_0 - \frac{c_+(\theta_0)}{p_+(\theta_0)} \lambda_+(\theta_0) r_2, \\ & v = v_0 - \frac{q_+(\theta_0)}{p_+(\theta_0)} \lambda_+(\theta_0) r_2, \\ & w_2 = -\lambda_+(\theta_0), \\ & r_2 \geq 0, \\ & \epsilon_2 = 0. \end{aligned} \quad \square$$

**PROOF** The first two statements follow directly from straightforward calculation. For  $\gamma_2^u(\theta_0, \phi_0, v_0)$  we restrict to the invariant set:  $\epsilon_2 = 0, w_2 = -\lambda_+$  and solve the resulting reduced system. ■

**Remark 10** The set  $\gamma_2^u(\theta_0, \phi_0, v_0)$  is  $\gamma^u(\theta_0, \phi_0, v_0)$  in (23) written in the chart  $\kappa_2$  for  $\epsilon = 0$ . □

Using  $\kappa_{21}$  (34) we transform  $z_1(\epsilon)$  to chart  $\kappa_2$ :

$$z_2(\epsilon) = \kappa_{21}(z_1(\epsilon)) = \{(\epsilon_2, w_2, \theta, \phi, v, r_2) \mid r_2 = \epsilon \nu^{-1}, w_2 = w_{1*} \nu + \mathcal{O}(\epsilon), \epsilon_2 = \nu\}.$$

Setting  $\epsilon = 0$  gives

$$z_2(0) = \kappa_{21}(z_1(0)) = \{(\epsilon_2, w_2, \theta, \phi, v, r_2) \mid r_2 = 0, w_2 = w_{1*} \nu, \epsilon_2 = \nu\}. \quad (39)$$

contained within the stable manifold of  $M_2$ . The forward flow of  $z_2(0)$  in (39) is described by

$$\begin{aligned} \epsilon_2(\tau) &= - \left( \frac{b(\theta_0, \phi_0)}{p_+(\theta_0)} + c_+ e^{\lambda_+ \tau} + c_- e^{\lambda_- \tau} \right)^{-1} \\ &= -c_+^{-1} e^{-\lambda_+ \tau} (1 + \mathcal{O}(e^{-\lambda_+ \tau} + e^{(\lambda_- - \lambda_+) \tau})), \\ w_2(t) &= - (c_+ \lambda_+ e^{\lambda_+ \tau} + c_- \lambda_- e^{\lambda_- \tau}) \left( \frac{b(\theta_0, \phi_0)}{p_+(\theta_0)} + c_+ e^{\lambda_+ \tau} + c_- e^{\lambda_- \tau} \right)^{-1} \\ &= -\lambda_+ (1 + \mathcal{O}(e^{-\lambda_+ \tau} + e^{(\lambda_- - \lambda_+) \tau})), \end{aligned} \quad (40)$$

for  $\tau \geq \tau_*$ , using (35), (34), and the asymptotics in (36).

We are now ready to prove Proposition 3.

#### 4.2.4 Proof of Proposition 3

We first use the following lemma:

**Lemma 3** *For  $\nu$  and  $\rho$  sufficiently small, then within  $U_2$  there exists a smooth transformation  $(\epsilon_2, w_2, \phi, v, r_2) \mapsto (\tilde{\phi}, \tilde{v})$  satisfying*

$$\begin{aligned}\tilde{\phi} &= \phi + \frac{c_+(\theta)}{p_+(\theta)} \lambda_+(\theta) r_2 + \mathcal{O}(r_2(w_2 + \lambda_+)), \\ \tilde{v} &= v + \frac{q_+(\theta)}{p_+(\theta)} \lambda_+(\theta) r_2 + \mathcal{O}(r_2(w_2 + \lambda_+) + \epsilon),\end{aligned}\tag{41}$$

which transforms (38) into

$$\begin{aligned}\epsilon'_2 &= -\epsilon_2 w_2, \\ w'_2 &= \epsilon_2 b(\theta, \tilde{\phi}) + p_+(\theta) [1 - \delta w_2] + w_2^2 + \mathcal{O}(\epsilon), \\ \theta' &= \epsilon \tilde{\phi}, \\ \tilde{\phi}' &= 0, \\ \tilde{v}' &= 0, \\ r'_2 &= -r_2 w_2.\end{aligned}\tag{42}$$

□

PROOF Replace  $r_2$  by  $\nu r_2$  in (38) and consider  $\nu$  small. Then  $\epsilon_2 = r_2 = 0$ ,  $w_2 = -\lambda_+$  is a saddle-type slow manifold for  $\nu$  small. The result then follows from Fenichel's normal form theory see e.g. [11]. The transformation simply straightens out the smooth fibers such that slow dynamics of  $(\theta, \tilde{\phi}, \tilde{v})$  becomes independent of the fast variables  $(\epsilon_2, w_2, r_2)$ . Using  $r_2 \epsilon_2 = \epsilon$  in the  $w_2$ -equation then gives the desired result.

Now we integrate (42) up until  $r_2(T) = \nu$  and obtain using (40)

$$\begin{aligned}\epsilon_2(T) &= \epsilon \nu^{-1} \\ w_2(T) &= -\lambda_+ + \mathcal{O}(\epsilon^c), \\ \theta(T) &= \theta_0 + \mathcal{O}(\epsilon \ln \epsilon^{-1}), \\ \tilde{\phi}(T) &= \tilde{\phi}_0, \\ \tilde{v}(T) &= \tilde{v}_0,\end{aligned}$$

with  $T = \mathcal{O}(\ln \epsilon^{-1})$ , for some  $c \in (0, 1)$  sufficiently small, as  $\epsilon \rightarrow 0$ . But then by (41) we obtain

$$\begin{aligned}\theta(T) &= \theta_0 + \mathcal{O}(\epsilon \ln \epsilon^{-1}), \\ \phi(T) &= \phi_0 - \frac{c_+(\theta_0)}{p_+(\theta_0)} \lambda_+(\theta_0) \nu + \mathcal{O}(\epsilon^c), \\ v(T) &= v_0 - \frac{q_+(\theta_0)}{p_+(\theta_0)} \lambda_+(\theta_0) \nu + \mathcal{O}(\epsilon^c),\end{aligned}$$

From here we return to (21) using (33) and integrate these initial conditions using regular perturbation theory up until the section  $\Pi$  (27). This gives (29) which completes the proof of Proposition 3.

### 4.3 Sticking

To continue (29) forward we have to follow the Filippov vector-field described in Proposition 1 cf. Lemma 1. This gives

$$\begin{aligned}\hat{y}' &= w, \\ w' &= \epsilon b(\theta, \phi) + S_w(\theta) [-\hat{y} - \delta w], \\ \theta' &= \epsilon \phi, \\ \phi' &= S_\phi(\theta) [-\hat{y} - \delta w],\end{aligned}$$

in terms of  $\hat{y}$  and the fast time  $\tau$ . Using regular perturbation theory we can from now on focus on  $\epsilon = 0$ . We therefore just consider

$$\begin{aligned}\hat{y}' &= w, \\ w' &= S_w(\theta) [-\hat{y} - \delta w], \\ \phi' &= S_\phi(\theta) [-\hat{y} - \delta w],\end{aligned}\tag{43}$$

with  $\theta = \theta_0$  constant. We integrate these equations with the initial conditions in (29) for  $\epsilon = 0$ :

$$\begin{aligned}\hat{y}(0) &= -\frac{p_+(\theta_0)}{q_+(\theta_0)\lambda_+(\theta_0)}v_0, \\ w(0) &= -\frac{p_+(\theta_0)}{q_+(\theta_0)}v_0, \\ \phi(0) &= \phi_0 - \frac{c_+(\theta_0)}{q_+(\theta_0)}v_0,\end{aligned}\tag{44}$$

up until  $[-\hat{y} - \delta w] = 0$  where by  $a \neq 0$  sticking ceases. Note this always occurs since

$$\hat{y}'' = w' > 0,$$

for  $[-\hat{y} - \delta w] > 0$ . Consider therefore the section

$$\Gamma = \{(\hat{y}, w, \phi) | \hat{y} + \delta w = 0\},$$

Then we obtain:

**Proposition 4** *There exists a smooth positive function  $e(\delta, \theta_0) > 0$  and a time  $\tau^* > 0$  such that:  $(\hat{y}(\tau^*), w(\tau^*), \phi(\tau^*)) \in \Gamma$  with*

$$\begin{aligned}\hat{y}(\tau^*) &= -\delta e(\delta, \theta_0)v_0, \\ w(\tau^*) &= e(\delta, \theta_0)v_0, \\ \phi(\tau^*) &= \phi_0 + \left\{ -\frac{c_+(\theta_0)}{q_+(\theta_0)} + \frac{S_\phi(\theta_0)}{S_w(\theta_0)} \left( e(\delta, \theta_0) + \frac{p_+(\theta_0)}{q_+(\theta_0)} \right) \right\} v_0,\end{aligned}$$

where  $(\hat{y}(\tau), w(\tau), \phi(\tau))$  is the solution of (43) with the initial conditions in (44).

The function  $e(\delta, \theta_0)$  satisfies the following asymptotics:

$$e(\delta, \theta_0) = -\frac{S_w(\theta_0) - p_+(\theta_0)}{q_+(\theta_0)S_w(\theta_0)}\delta^{-2} (1 + \mathcal{O}(\delta^{-2} \ln \delta^{-4})) \quad \text{for } \delta \gg 1,$$

$$e(\delta, \theta_0) = -\frac{\sqrt{p_+(\theta_0)(p_+(\theta_0) - S_w(\theta_0))}}{q_+(\theta_0)} \left( 1 - \frac{\sqrt{S_w(\theta_0)}}{2} \left( \pi - \arctan \left( \sqrt{-\frac{S_w(\theta_0)}{p_+(\theta_0)}} \right) \right) \delta + \mathcal{O}(\delta^2) \right) \quad \text{for } \delta \ll 1. \quad \square$$

**PROOF** The existence of  $\tau^*$  is obvious. The linearity in  $v_0$  follows from linearity of (43). Since  $\dot{y} = w$  we have  $e > 0$ . The  $\phi$ -equation follows from the fact that

$$\phi' = \frac{S_\phi(\theta)}{S_w(\theta)} w'.$$

To obtain the asymptotics we first solve (43) with  $\delta \neq \frac{2}{\sqrt{S_w(\theta_0)}}$  (which is true for  $\delta \gg 1$  and  $\delta \ll 1$ ). Simple calculations show that

$$e(\delta, \theta_0) = \frac{\xi_+}{\xi_-} (\lambda_+ - \xi_-) \frac{p_+}{q_+ \lambda_+} e^{\xi_+ \tau^*}, \quad (45)$$

suppressing the dependency on  $\theta_0$  on the right hand side, where

$$\xi_\pm = -\frac{\delta S_w}{2} \pm \frac{1}{2} \sqrt{\delta^2 S_w^2 - 4S_w},$$

and  $\tau^*$  being the least positive solution of

$$e^{(\xi_+ - \xi_-)\tau^*} = \frac{\xi_-^2 (\lambda_+ - \xi_+)}{\xi_+^2 (\lambda_+ - \xi_-)}.$$

For  $\delta \gg 1$  the eigenvalues  $\xi_\pm$  are real and negative. Hence

$$\tau^* = \frac{1}{\xi_+ - \xi_-} \ln \left( \frac{\xi_-^2 (\lambda_+ - \xi_+)}{\xi_+^2 (\lambda_+ - \xi_-)} \right).$$

Now using

$$\xi_+ = -S_w \delta (1 + \mathcal{O}(\delta^{-2})), \quad \xi_- = \frac{S_w}{\xi_-} = -\delta^{-1} (1 + \mathcal{O}(\delta^{-1})),$$

and

$$\lambda_+ = -p_+ \delta (1 + \mathcal{O}(\delta^{-2})),$$

we obtain

$$\xi_+ \tau^* = \mathcal{O}(\delta^{-2} \ln \delta^{-4}),$$

and hence

$$e(\delta, \theta_0) = -\frac{S_w - p_+}{q_+ S_w} \delta^{-2} (1 + \mathcal{O}(\delta^{-2} \ln \delta^{-4})),$$

as  $\delta \rightarrow \infty$ .

Finally, for  $\delta \ll 1$  then the eigenvalues  $\xi_{\pm}$  are complex conjugated with negative real part. This gives

$$\tau^* = \frac{2i}{\xi_+ - \xi_-} (\phi - \pi n), \quad \phi = \arg((\lambda_+ - \xi_+) \xi_-^2) > 0, \quad n = \lfloor \phi/\pi \rfloor.$$

Using the asymptotics of  $\xi_{\pm}$  and  $\lambda_+$  we obtain

$$\tau^* = \frac{\pi - \arctan\left(\sqrt{-\frac{S_w}{p_+}}\right)}{\sqrt{S_w}} - \frac{1}{2}\delta(1 + \mathcal{O}(\delta)),$$

and then

$$e(\delta, \theta_0) = -\frac{\sqrt{p_+(p_+ - S_w)}}{q_+} \left(1 - \frac{\sqrt{S_w}}{2} \left(\pi - \arctan\left(\sqrt{-\frac{S_w}{p_+}}\right)\right)\right) \delta + \mathcal{O}(\delta^2). \quad \blacksquare$$

**Remark 11** The critical value  $\delta = \frac{2}{\sqrt{S_w(\theta_0)}}$  gives a double root of the characteristic equation. Also it reduces to  $\delta_{crit} = 2$ , when  $\theta_0 = \frac{\pi}{2}$  for the classical Painlevé problem, as expected (see section 2.2).  $\square$

#### 4.4 Lift off

Beyond  $\Gamma$  we have  $\hat{F}_N \equiv 0$  and lift off occurs. For  $\epsilon = 0$  we obtain

$$\hat{y}' = w$$

and  $w' = \theta' = \phi' = v' = 0$ . By Proposition 4, regular perturbation theory and simple algebraic manipulations using (8) we obtain the desired result in Theorem 1. In terms of the original (slow) time  $t$  it follows that the time of IWC is of order  $\mathcal{O}(\epsilon \ln \epsilon^{-1})$ . As  $\epsilon \rightarrow 0$  the IWC occurs instantaneously as desired.

## 5 Conclusions

We have considered the problem of a rigid body, subject to a unilateral constraint, in the presence of Coulomb friction. We have focused on the Painlevé paradox known as the inconsistent case where the classic rigid body formalism yields no solution. Our approach was to regularize the problem by assuming compliance at the point of contact. This leads to a slow-fast system, where the small parameter  $\epsilon$  is the inverse of the square root of the compliance stiffness. We then solve the problem using geometric singular perturbation theory and blowup.

Like other authors, we found that the fast solution (or boundary layer) is unstable in the inconsistent case. But we exploit this fact by following its unstable direction until the rod sticks. We solve the problem both in the stick phase and in the lift off phase. We have also shown how to match solutions obtained by scalings used by previous authors.

Our results are presented for arbitrary values of the compliance damping and we are able to give explicit asymptotic expressions in the limiting cases of small and large damping, all for a large class of rigid body, including the case of the classical Painlevé example in Fig. 1.

The aim of our paper is to show the power of geometric singular perturbation theory and blowup. Given a general class of rigid body and a general class of normal reaction, we have been able to derive an explicit connection between the initial horizontal velocity of the body and its lift-off vertical velocity, for arbitrary values of the compliance damping, as a function of the initial orientation of the body.

## References

- [1] Le Suan An. The Painlevé paradoxes and the law of motion of mechanical systems with Coulomb friction. *Prikl. Math. Mekh.*, 54:430–438, 1990.
- [2] A. Blumenthals, B. Brogliato, and F. Bertails-Descoubes. The contact problem in Lagrangian systems subject to bilateral and unilateral constraints, with or without sliding Coulomb’s friction: a tutorial. *Multibody Syst. Dyn.*, 38:43–76, 2016.
- [3] R.M. Brach. Impacts coefficients and tangential impacts. *ASME J. Applied Mechanics*, 64:1014–1016, 1997.
- [4] B. Brogliato. *Nonsmooth mechanics*. Springer, London, 2nd edition, 1999.
- [5] A.R. Champneys and P. Várkonyi. The Painlevé paradox in contact mechanics. *IMA J. Applied Math.*, 81:538–588, 2016.
- [6] G. Darboux. Étude géométrique sur les percussions et le choc des corps. *Bulletin des Sciences Mathématiques et Astronomique, 2e serie*, 4:126–160, 1880.
- [7] P. E. Dupont and S. P. Yamajako. Stability of frictional contact in constrained rigid-body dynamics. *IEEE Trans. Robotics Automation*, 13:230–236, 1997.
- [8] A.F. Filippov. *Differential Equations with Discontinuous Righthand Sides*. Mathematics and its Applications. Kluwer Academic Publishers, 1988.
- [9] F. Génot and B. Brogliato. New results on Painlevé paradoxes. *European Journal of Mechanics A/Solids*, 18:653–677, 1999.
- [10] A.P. Ivanov. On the correctness of the basic problem of dynamics in systems with friction. *Prikl. Math. Mekh.*, 50:547–550, 1986.
- [11] C.K.R.T. Jones. *Geometric Singular Perturbation Theory, Lecture Notes in Mathematics, Dynamical Systems (Montecatini Terme)*. Springer, Berlin, 1995.



- [12] J. B. Keller. Impact with friction. *ASME J. Applied Mechanics*, 53:1–4, 1986.
- [13] K. Uldall Kristiansen and S. J. Hogan. On the use of blowup to study regularizations of singularities of piecewise smooth dynamical systems in  $\mathbb{R}^3$ . *SIAM Journal on Applied Dynamical Systems*, 14(1):382–422, 2015.
- [14] K. Uldall Kristiansen and S. J. Hogan. Regularizations of two-fold bifurcations in planar piecewise smooth systems using blowup. *SIAM Journal on Applied Dynamical Systems*, 14(4):1731–1786, 2015.
- [15] M. Krupa and P. Szmolyan. Extending geometric singular perturbation theory to non-hyperbolic points - fold and canard points in two dimensions. *SIAM Journal on Mathematical Analysis*, 33(2):286–314, 2001.
- [16] C. Kuehn. *Multiple Time Scale Dynamics*. Springer-Verlag, Berlin, 2015.
- [17] L. Lecornu. Sur la loi de Coulomb. *Comptes Rendu des Séances de l'Academie des Sciences*, 140:847–848, 1905.
- [18] R. Leine, B. Brogliato, and H. Nijmeijer. Periodic motion and bifurcations induced by the Painlevé paradox. *European Journal of Mechanics A/Solids*, 21:869–896, 2002.
- [19] C. Liu, Z. Zhao, and B. Chen. The bouncing motion appearing in a robotic system with unilateral constraint. *Nonlinear Dynamics*, 49:217–232, 2007.
- [20] N. H. McClamroch. A singular perturbation approach to modeling and control of manipulators constrained by a stiff environment. In *Proc. 28th Conf. Decision Contr.*, pages 2407–2411, December 1989.
- [21] Yu. I. Neimark and N. A. Fufayev. The Painlevé paradoxes and the dynamics of a brake shoe. *J. Applied Math. Mech.*, 59:343–352, 1995.
- [22] Y. Or. Painlevé's paradox and dynamic jamming in simple models of passive dynamic walking. *Regular and Chaotic Dynamics*, 19:64–80, 2014.
- [23] Y. Or and E. Rimon. Investigation of Painlevé's paradox and dynamic jamming during mechanism sliding motion. *Nonlinear Dynamics*, 67:1647–1668, 2012.
- [24] P. Painlevé. Sur les loi du frottement de glissement. *Comptes Rendu des Séances de l'Academie des Sciences*, 121:112–115, 1895.
- [25] P. Painlevé. Sur les loi du frottement de glissement. *Comptes Rendu des Séances de l'Academie des Sciences*, 141:401–405, 1905.
- [26] P. Painlevé. Sur les loi du frottement de glissement. *Comptes Rendu des Séances de l'Academie des Sciences*, 141:546–552, 1905.
- [27] P. Song, P. Kraus, V. Kumar, and P. E. Dupont. Analysis of rigid-body dynamic models for simulation of systems with frictional contacts. *ASME J. Applied Mechanics*, 68:118–128, 2001.

- [28] D. E. Stewart. Rigid-body dynamics with friction and impact. *SIAM Review*, 42:3–39, 2000.
- [29] E. V. Wilms and H. Cohen. Planar motion of a rigid body with a friction rotor. *ASME J. Applied Mechanics*, 48:205–206, 1981.
- [30] E. V. Wilms and H. Cohen. The occurrence of Painlevé’s paradox in the motion of a rotating shaft. *ASME J. Applied Mechanics*, 64:1008–1010, 1997.
- [31] Z. Zhao, C. Liu, B. Chen, and B. Brogliato. Asymptotic analysis and Painlevé’s paradox. *Multibody Syst. Dyn.*, 35:299–319, 2015.
- [32] Z. Zhao, C. Liu, W. Ma, and B. Chen. Experimental investigation of the Painlevé paradox in a robotic system. *ASME J. Applied Mechanics*, 75:041006, 2008.